Supplementary material

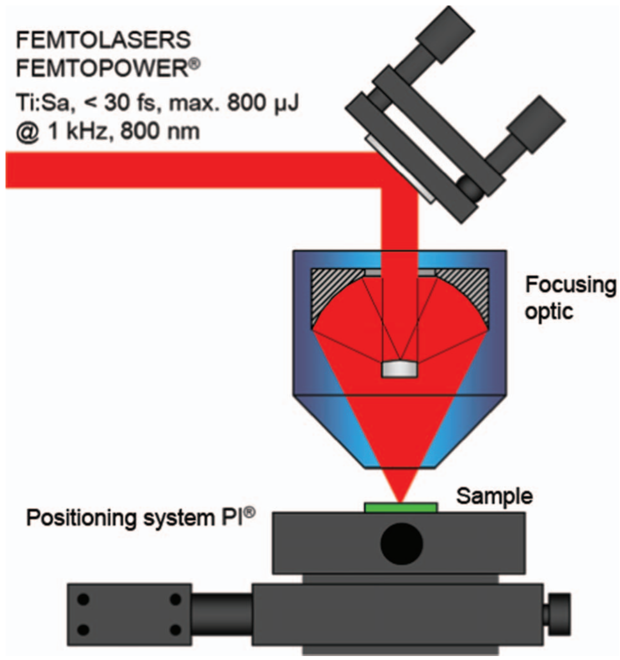

Figure S1. Schematic sketching of the femtosecond ablation system.

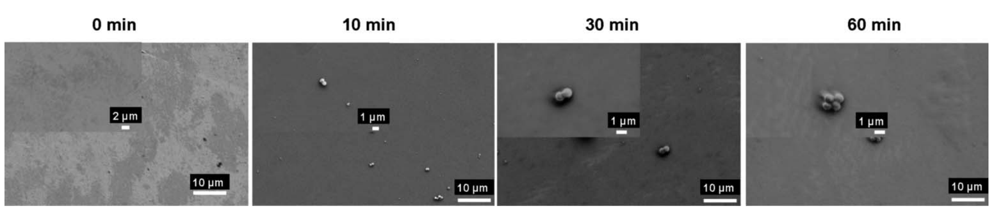

Figure S2. Representative SEM images of *S. aureus* CIP 65.8 adhesion on polished and lotus-like Ti after incubation for 0 min, 10 min, 30 min and 60 min.

Table S1. Number of attached cells and biovolume of produced EPS on as-received and lotus-like Ti surfaces.

	Retained cells[a] $\times 10^5$ [number of cells mm^{-2}]		Biovolume of EPS production (μm)	
Bacterial strains	As-received	Lotus-like	As-received	Lotus-like
S. aureus CIP 65.8[T]	0.47 ± 0.06	11.09 ± 1.51	2.33 ± 0.49	8.69 ± 1.96
S. aureus ATCC 25923	1.58 ± 0.80	2.44 ± 0.56	3.00 ± 0.60	6.30 ± 2.80
S. epidermidis ATCC 14990[T]	1.72 ± 0.46	8.73 ± 2.70	4.50 ± 1.00	7.00 ± 1.47
Planococcus maritimus KMM 3738	<dl[a]	0.53 ± 0.13	<dl	0.20 ± 0.09

[a]Below detection limit.

Table S2. Extended set of surface roughness parameters of control and lotus-like Ti surfaces over scanning areas of 10 μm × 10 μm and 5 μm × 5 μm.

	Surfaces	S_a (nm)	S_q (nm)	S_{max} (nm)	S_{sk}	S_{ku}	S_{dr} (%)
10 μm × 10 μm	As-received Ti	2.12 ± 0.34	4.68 ± 0.76	120.60 ± 19.58	8.63 ± 1.40	137.13 ± 22.26	0.13 ± 0.02
	Lotus–like Ti	257.74 ± 41.84	328.74 ± 53.37	2392.60 ± 388.42	−0.43 ± 0.07	3.03 ± 0.49	42.70 ± 6.93
5 μm × 5 μm	As-received Ti	1.01 ± 0.16	2.26 ± 0.37	71.68 ± 11.64	10.99 ± 1.78	211.05 ± 34.26	0.24 ± 0.02
	Lotus–like Ti	96.38 ± 15.65	121.58 ± 19.74	945.37 ± 153.47	−0.07 ± 0.01	3.00 ± 0.49	50.09 ± 8.13

Table S3. Adhesion kinetics of the polished and lotus-mimicked superhydrophobic Ti surfaces by *S. aureus* CIP 65.8.

Incubation time	Retained cells[a] × 10^4 [number of cells mm^{-2}]		Biovolume of EPS production (μm)	
	As-received	Lotus-like	As-received	Lotus-like
10 min	<dl[b]	0.3 ± 0.07	<dl	1.1 ± 0.2
30 min	<dl	9.1 ± 0.9	<dl	1.4 ± 0.8
60 min	<dl	12.7 ± 4.3	<dl	1.5 ± 0.6

[a]Cell densities have estimated errors of ~15–20% due to local variability in the surface coverage; [b]below detection limit.

Ti surface topography and wettability

The surface topography at both micro- and nano-metric scale is evidenced to place an influence upon the adhesive behaviours of bacteria (Anselme et al. 2010; Ploux et al. 2010; Rizzello et al. 2011; Webb et al. 2011). In order to understand surface topography at the micro/nano-scale, three dimensional topography of as-received and lotus-like Ti over 10 μm × 10 μm is shown in Figure S2 and a comprehensive description of surface topography is evaluated by several surface parameters in Table S2. After femtosecond laser ablation, there was a significant change in the surface topography of the as-received Ti surfaces. As shown in Figure S2, lotus-like Ti surfaces exhibited deep valleys with a depth of 3.4 μm and large plateaux with the width of 10 μm to 20 μm. On the top of these plateaux, there is a second tier of nanotopography with undulations of 200 nm. This two-tier topography was formed spontaneously under femtosecond laser irradiation. This 'self-organisation' effect was reported previously after femtosecond laser ablation (Vorobyev et al. 2007; Fadeeva et al. 2011). In Table S1, the S_a, S_q and S_{max} of lotus-like Ti surfaces are considerably greater than those of as-received Ti on both the 10 μm × 10 μm and 5 μm × 5 μm scanning areas. The developed surface area ratio (ie the ratio of surface area to projected area) of lotus-like Ti surfaces (S_{dr} = 42.70% and 50.09% respectively for 10 μm × 10 μm and 5 μm × 5 μm scanning areas) is significantly higher than as-received Ti (S_{dr} = 0.13% and 0.24% respectively for 10 μm × 10 μm and 5 μm × 5 μm scanning areas). To provide sufficient information on the surface architecture, skewness (S_{sk}) and kurtosis (S_{ku}) were also utilised to describe the distribution of heights. On both the 10 μm × 10 μm and 5 μm × 5 μm scanning areas, as-received Ti surfaces had S_{sk} values of 8.63 and 10.99 respectively, and S_{ku} values of 137.13 and 211.05 over the same scanning areas, indicative of a highly uneven distribution of peaks and valleys and a complicated surface architecture. In contrast, lotus-like Ti surfaces have S_{sk} values close to 0 and S_{ku} values close to 3, highlighting the relatively symmetric distribution of peaks and valleys across the analysed surfaces.

The wettability of lotus-like Ti surfaces was examined in a previous study in which the water contact angle was 166° (Fadeeva et al. 2011). It can be explained by the Cassie-Baxter model of wettability, in which the air component entrapped between micro/nano-structures enhances the natural surface wettability, according to:

$$\cos\theta = f_1(\cos\theta_1 + 1) - 1$$

where θ is the composite contact angle of the heterogeneous surface, f_1 is the area fraction of surface component of Ti and θ_1 is the contact angle on the projected surface of Ti (Cassie and Baxter 1944).

References

Anselme K, Davidson P, Popa AM, Giazzon M, Liley M, Ploux L. 2010. The interaction of cells and bacteria with surfaces structured at the nanometre scale. Acta Biomaterial 6:3824–3846.

Cassie ABD, Baxter S. 1944. Wettability of porous surfaces. Trans Faraday Soc 40:546–551.

Fadeeva E, Truong VK, Stiesch M, Chichkov BN, Crawford RJ, Wang J, Ivanova EP. 2011. Bacterial retention on superhydrophobic titanium surfaces fabricated by femtosecond laser ablation. Langmuir. 27:3012–3019.

Ploux L, Ponche A, Anselme K. 2010. Bacteria/material interfaces: role of the material and cell wall properties. J Adhes Sci Technol 24:2165–2201.

Rizzello L, Sorce B, Sabella S, Vecchio G, Galeone A, Brunetti V, Cingolani R, Pompa PP. 2011. Impact of nanoscale topography on genomics and proteomics of adherent bacteria. ACS Nano 5:1865–1876.

Vorobyev AY, Makin VS, Guo C. 2007. Periodic ordering of random surface nanostructures induced by femtosecond laser pulses on metals. J Appl Phys 101:no. 034903.

Webb HK, Hasan J, Truong VK, Crawford RJ, Ivanova EP. 2011. Nature inspired structured surfaces for biomedical applications. Curr Med Chem 18:3367–3375.